

Protection properties of conversion coatings based on nitrates for resorbable Mg alloy

Katarzyna CESARZ-ANDRACZKE*

Department of Engineering Materials and Biomaterials, Faculty of Mechanical Engineering,
Silesian University of Technology, ul. Konarskiego 18A, 44-100 Gliwice, Poland

Abstract. In this work, conversion coatings based on nitrates $\text{Ca}(\text{NO}_3)_2$ and $\text{Zn}(\text{NO}_3)_2$ were produced on the surface of $\text{MgZn}_{49}\text{Ca}_4$ to protect against corrosion. The main aim of this study was to prepare dense and uniform coatings using a conversion method (based on nitrates $\text{Ca}(\text{NO}_3)_2$ and $\text{Zn}(\text{NO}_3)_2$) for resorbable Mg alloys. The scientific goal of the work was to determine the pathway and main degradation mechanisms of samples with nitrate-based coatings as compared with an uncoated substrate. Determining the effect of the coatings produced on the Mg alloy was required to assess the protective properties of Mg alloy-coating systems. For this purpose, the morphology and chemical composition of coated samples, post corrosion tests and structural tests of the substrate were performed (optical microscopy, SEM/EDS). Immersion and electrochemical tests of samples were also carried out in Ringer's solution at 37°C. The results of immersion and electrochemical tests indicated lower corrosion resistance of the substrate as compared with coated samples. The hydrogen evolution rate of the substrate increased with the immersion time. For coated samples, the hydrogen evolution rate was more stable. The ZnN coating (based on $\text{Zn}(\text{NO}_3)_2$) provides better corrosion protection because the corrosion product layer was uniform, while the sample with a CaN coating (based on $\text{Ca}(\text{NO}_3)_2$) displayed clusters of corrosion products. It was found that pitting corrosion on the substrate led to the complete disintegration and non-uniform corrosion of the coated samples, especially the CaN sample, due to the unevenly-distributed products on its surface.

Key words: magnesium alloys; protection coatings; hydrogen evolution; corrosion behavior.

1. Introduction

One of the directions in the search for new orthopedic implant materials is the investigation of resorbable biomaterials. Biocompatible resorbable implants eliminate the need for a second implant surgery and reduce post-operative costs, including the costs of patient rehabilitation. New biocompatible resorbable short-term orthopedic implants are based on the idea that implant materials should contain elements present in the human body [1, 2]; however, it is difficult to guarantee only a small variation in the strength and dimensions of implants, which either lack or have a low degradation rate during bone concretion. The volume of hydrogen released by implant degradation should not exceed approx. 1 ml/h because this is the hydrogen absorption limit of human tissues [3]. In addition, the problem with new resorbable alloys based on Ca, Zn, and Mg is that they may exceed the daily limit for elements introduced into the body.

Generally, two research directions have been used to reduce the degradation rate during bone concretion: modification of the chemical composition of Ca, Mg, and Zn alloys or the use of slowly degradable protective coatings. The use of protective coatings can increase the corrosion resistance of biocompatible Ca, Mg, and Zn alloys, which are more widely studied in the literature. Previously, ceramic coatings such as oxides [4–9]

and phosphates [10–12] have been used to increase the corrosion resistance of magnesium alloys. Most proposed ceramic coatings are non-resorbable. In addition, polymer coatings have been tested as resorbable coatings, including PLA, PLGA and copolymers [13, 14]. Composite coatings increase the corrosion resistance of magnesium alloys examined by several researchers, including oxide-phosphate [15, 16] and ceramic-polymer [17, 18] coatings. In the literature, different conversion coatings (e.g. those based on MgP, ZnP, CaP or Zn-Ca-P) on Mg alloy substrates have been used to compare the corrosion resistance and biocompatibility of these coatings [19–22]. Producing conversion layers does not require sophisticated equipment, and they can be obtained by chemical methods, e.g. dip coating, or electrochemical methods, e.g. electrodeposition. Conversion coatings are produced on the surface of metallic materials to provide corrosion protection. The protective coatings, mainly conversion coatings, are used to improve the corrosion resistance of metals such as zinc [23].

The main aim of this study was to prepare dense and uniform coatings using a nitrate-based conversion method for resorbable Mg alloys. The scientific goal of the work was to determine the course and main degradation mechanisms of samples with nitrate-based coatings as compared with an uncoated substrate sample. Determining the effect of the coatings produced on the $\text{MgZn}_{49}\text{Ca}_4$ alloy was necessary to assess the Mg alloy-coating systems manufactured in terms of the protective properties of manufactured materials.

The $\text{MgZn}_{49}\text{Ca}_4$ alloy was selected for the study because own studies and a literature review have demonstrated that the alloying system of Mg – Zn – Ca may offer a very attractive

*e-mail: Katarzyna.Cesarz-Andraczke@polsl.pl

Manuscript submitted 2020-09-01, revised 2020-12-03, initially accepted for publication 2020-12-03, published in February 2021

combination of high strength and simultaneous high ductility; $R_p > 200$ MPa, $R_m > 250$ MPa, $A > 20\%$.⁴

In addition, Zn and Ca are both essential elements in the human body and, as alloying element in Mg, they are known to positively influence bone healing and cell reactions [24].

The chemical composition of the alloy for testing, such as: Zn = 49% wt and Ca = 4% wt, was selected based on the Mg-Zn-Ca phase system [25] in order to obtain a large proportion of the Ca₂Mg₆Zn₃ phase in the structure (Fig. 1). In work [26], it was found that the Ca₂Mg₆Zn₃ phase increases the microhardness, strength and ductility of alloys.

Mechanical properties studies are not presented in this work. However, microhardness of the MgZn₄₉Ca₄ alloy was tested. The results are as follows: 186 HV, 190 HV, 179 HV, 181 HV and 188HV. The average microhardness is therefore 185 HV. It was found in [26] that the MgZn₃₅Ca₂ alloy, which was characterized by microhardness of about 164 HV, is expected to bear the load during long-term implantation.

The chemical composition of the layering solution was selected to contain the nitrate components of the alloy. Safety data sheets of calcium nitrate and zinc nitrate are classified as non-toxic substances for human organs, not corrosive or allergenic. Calcium and zinc nitrate are likewise not classified as being germ cell mutagenic, carcinogenic or as a reproductive toxicant.

2. Material and methods

The MgZn₄₉Ca₄ alloys were produced by melting Mg, Zn and Ca in an induction furnace. The following elements with high purity were used: Mg 99.95%, Zn 99.98% and Ca 99.99%. The elements, in the following order: Zn, Mg, Ca, were melted at a temperature of about 650°C in a ceramic crucible with a protective atmosphere (argon). The order of adding elements to the crucible was determined in terms of the melting point of the element – from the lowest to the highest. The cooling of the alloy takes place along with the furnace. The MgZn₄₉Ca₄ (wt.%) samples with a size of 35×25×5 mm were used as a substrate for coatings. The substrate surface was mechanically ground up to 600 grit, cleaned using distilled water and ethanol, and then dried in the open air. To prepare nitrate-based coatings, the MgZn₄₉Ca₄ alloy samples were immersed in a beaker containing an RCaN and RZnN solution (Table 1) over 2 h. Samples were annealed in an electric furnace at 150°C for 2 h.

Table 1
Chemical composition of solution (with designations)
used to prepare coatings

Name of solution	Qualitative chemical composition of the solution	Designation of sample
RCaN	0.2M Ca(NO ₃) ₂ · 4H ₂ O + + 1M NaOH + distilled water + + annealing (150°C, 2 h)	CaN
RZnN	0.2M Zn(NO ₃) ₂ * 6H ₂ O Ca(NO ₃) ₂ + + 1M NaOH + distilled water + + annealing (150°C, 2 h)	ZnN

Both solutions (RCaN, RZnN, Table 1) were prepared at room temperature. The ingredients were mixed until a homogeneous solution was obtained. Chemicals of analytical-grade purity (produced by Chempur) were used to prepare solutions for all samples.

The structure of the substrate was studied using light microscopy (Zeiss) and Axiovision Rel. 4.4 software. To identify the location of phases in the substrate, scanning electron microscopy (SEM Supra 35 Carl Zeiss) with an EDS analyzer was used. The structure of the coatings, particle morphology (obtained by drying the RCaN and RZnN solutions) and post-corrosion tests were observed by means of scanning electron microscopy (SEM Supra 35 Carl Zeiss). After 96 h of immersion in Ringer's solution, the corrosion products and chemical composition of the corroded surfaces were examined using an EDS analyzer.

The immersion tests and measurements of released hydrogen volume were carried out in Ringer's solution (8.6 g/dm³ NaCl, 0.3 g/dm³ KCl, 0.48 g/dm³ CaCl₂ · 6H₂O) for 96 h. The hydrogen evolution volumes were measured at 37°C using an experimental station developed by the authors. The experimental station consists of: a thermostat, a glass beaker with Ringer's solution with a sample inside, a burette with a shut-off valve, a vessel with a bottom tube for balancing the pressure in the burette with atmospheric pressure, a venting valve and a silicone stopper. The evolved hydrogen gas was directed to the burette through a funnel, which in turn decreased the level of the solution in the burette. Changes in the solution level in the burette after alignment with the level of solution from the vessel with a tube were performed at 24 h intervals. It should be noted that the experimental station was used to determine only the volume of evolved hydrogen. Some hydrogen gas was absorbed by magnesium alloys, and this amount was undetermined.

The corrosion behavior of alloys was studied by electrochemical measurements using an Autolab 302N workstation controlled by NOVA 1.11 software. The corrosion studies were conducted in Ringer's solution at 37°C using a three-electrode cell. The electrodes included a sample (uncoated MgZn₄₉Ca₄ alloy or coated samples) as the working electrode, a counter platinum electrode and an AgCl reference electrode. Before measurements, the uncoated MgZn₄₉Ca₄ alloy was polished with grinding paper with 1200 grit and subsequently cleaned in acetone. Potentiodynamic measurements involved recording the open circuit potential (E_{OCP}) for 1 h and determining the electrochemical curves.

3. Results

Structural studies of the Mg₄₉Zn₄Ca alloy are presented in Fig. 1. Based on the Mg-Zn-Ca phase system [25], the alloy structure included three phases: Mg, Ca₂Mg₆Zn₃ and Mg₁₂Zn₁₃. Based on qualitative analysis results (EDX), the probable distribution of these phases in the Mg₄₉Zn₄Ca alloy's structure was determined (Fig. 2).

The SEM images of CaN and ZnN coatings on the Mg₄₉Zn₄Ca alloy and their chemical composition analy-

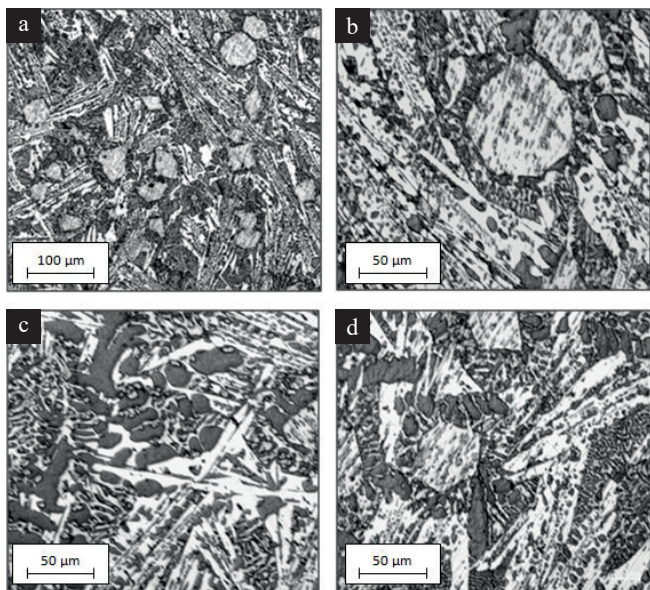


Fig. 1. Structure of Mg49Zn4Ca alloy at 100× (a) and 500× (b–d) magnification

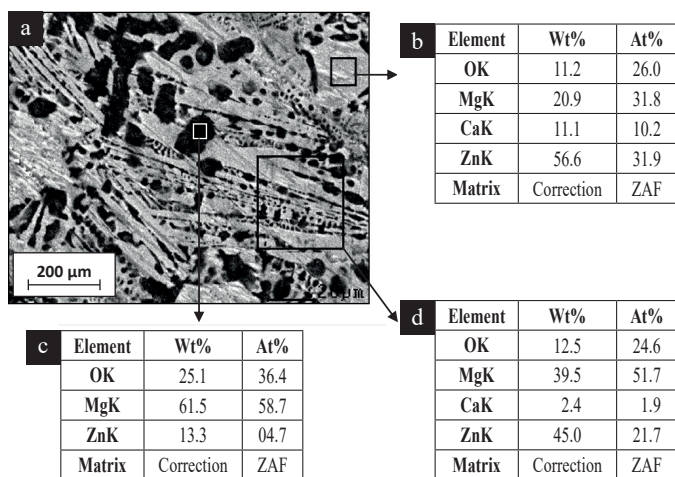


Fig. 2. SEM images (a) of Mg49Zn4Ca alloy structure and EDX chemical composition analysis of Ca2Mg6Zn3 (b), Mg (c) and Mg12Zn13 (d) phases

sis (EDX) are shown in Fig. 3 and Fig. 4, respectively. Both coatings were compact; however, the morphology of the CaN coating consisted of crystal-like elements (Fig. 3b). The EDX analysis of the CaN sample indicated the presence of mainly O, Na, Mg, Zn and Ca (from the substrate). On the surface, ZnN peaks of O, Zn, Mg and Ca were identified.

The SEM images of powder particles obtained by drying the RCaN solution (a) and drying the RZnN solution (c) along with the EDX chemical composition analysis are shown in Fig. 5. In both samples, powder particles were agglomerated. EDX analysis indicated the presence of Na and O in the RCaN sample, and Zn and O elements in the RZnN sample. This showed that the CaN and ZnN coatings consisted of Na, O and Zn, O elements, respectively.

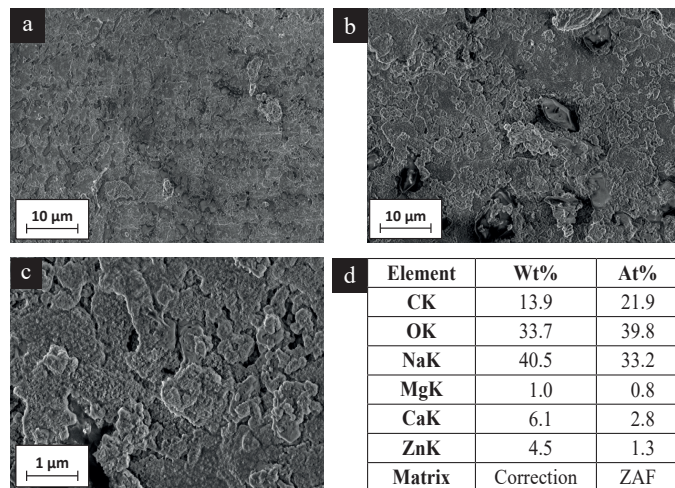


Fig. 4. SEM images (a, b, c) of ZnN coating on Mg49Zn4Ca alloy and EDX chemical composition analysis (d)

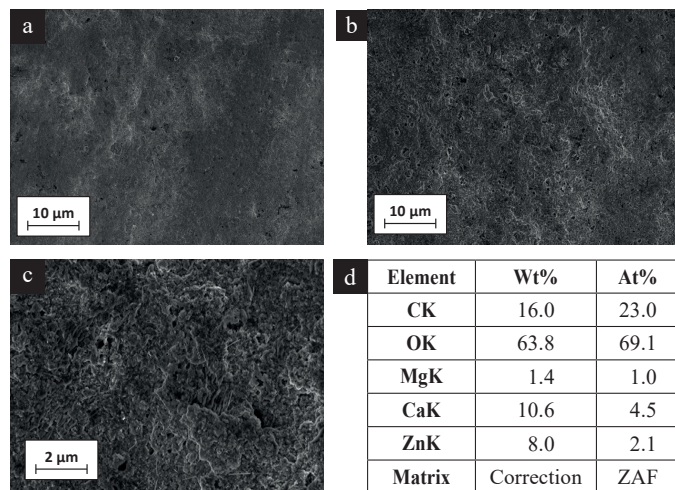


Fig. 4. SEM images (a, b, c) of ZnN coating on Mg49Zn4Ca alloy and EDX chemical composition analysis (d)

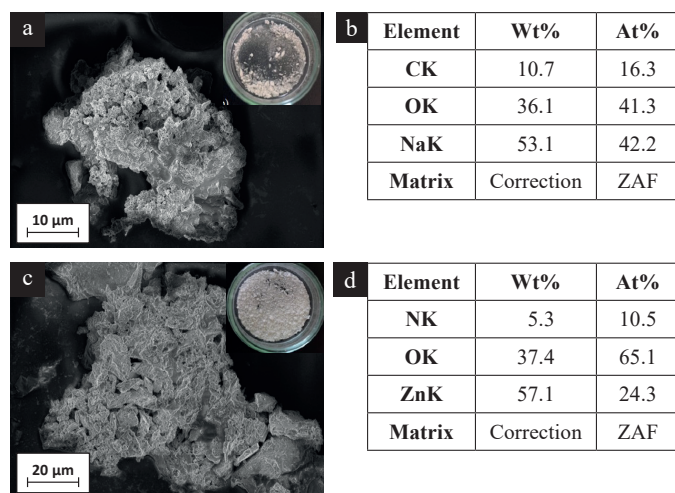


Fig. 5. SEM images of powder particles obtained by drying the RCaN (a) and RZnN solutions (c), and the EDX chemical composition analysis (b), (d), respectively

The results of immersion tests in Ringer's solution at 37°C are shown in Fig. 6. After 96 h immersion, the volume of evolved hydrogen (Fig. 6a) was about 7.1 ml/cm², 4.1 ml/cm², 3.4 ml/cm² for the Mg49Zn4Ca alloy substrate, Mg49Zn4Ca alloy + CaN coating, and Mg49Zn4Ca alloy + ZnN coating, respectively. The hydrogen evolution rate (Fig. 6b) of the substrate increased with the immersion time. For coated samples, the hydrogen evolution rate was stable at ≈ 0.4 ml/cm²/h for the CaN coating and ≈ 0.3 ml/cm²/h for the ZnN coating.

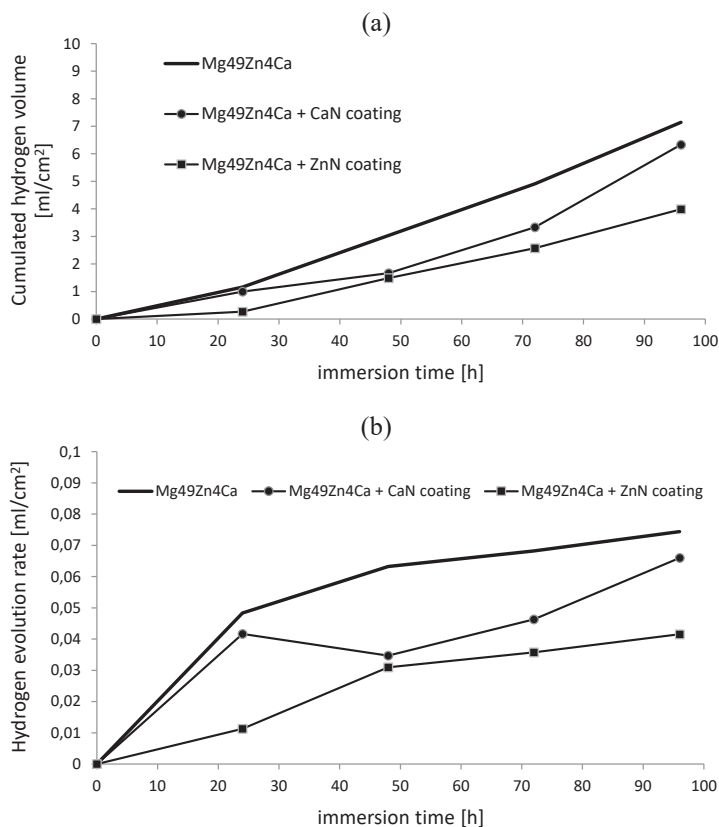


Fig. 6. Results of immersion tests: a) cumulative hydrogen volume, b) hydrogen evolution rate of the substrate and coated samples immersed in Ringer's solution at 37°C

The substrate and coated samples were studied by means of electrochemical measurements. The potentiodynamic measurements (a) and changes in the open-circuit potential as a function of immersion time (b) in Ringer's solution at 37°C are shown in Fig. 7. The cathodic part of the potentiodynamic curve of the Mg49Zn4Ca alloy was located in the high current range, which indicated high cathodic activity (Fig. 7a). The cathodic part of the potentiodynamic curve of the coated samples was located in a lower current range, which indicated lower cathodic activity than for the substrate. In addition, the potentiodynamic curves obtained for coated samples in relation to the potentiodynamic curves of the substrate moved to more positive potentials, which indicates an increase in corrosion resistance. The highest E_{OCP} fluctuation of 1 h for the substrate was observed (Fig. 7b), while the open circuit potential of the coated samples

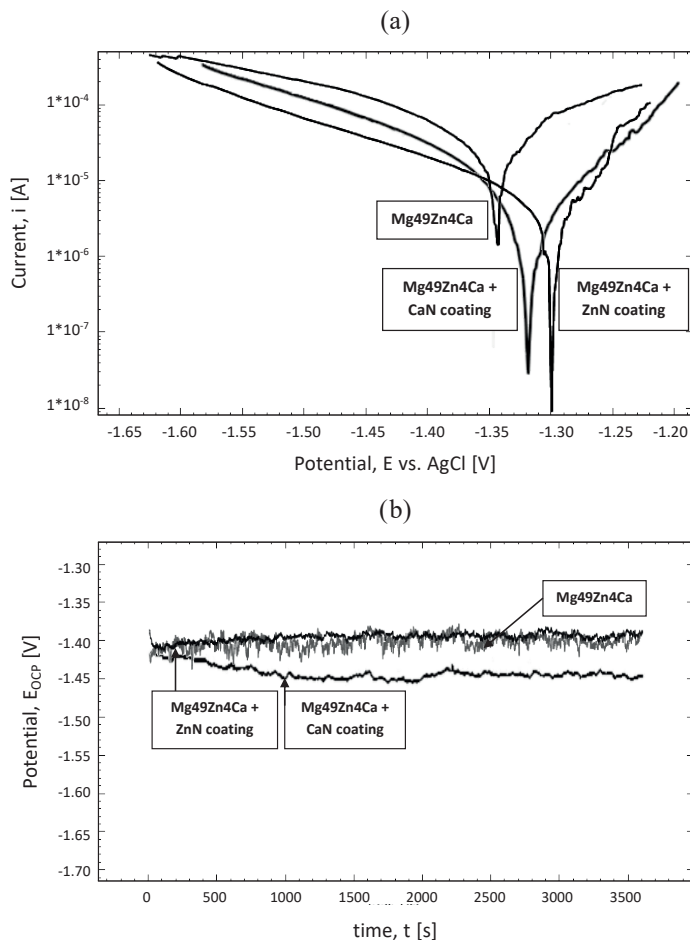


Fig. 7. Potentiodynamic curves (a) and changes in the open-circuit potential as a function of time in Ringer's solution at 37°C for samples studied

was more stable after 1 h of immersion. The results of the open circuit potential measurements of the Mg49Zn4Ca alloy with CaN moved to the negative direction after 10 min and remained in the range of -1.4 to -1.45 after immersion for 1 h. The E_{OCP} determined for the ZnN-coated sample was similar to the E_{OCP} of the substrate.

The SEM images of residual Mg49Zn4Ca after immersion tests in Ringer's solution at 37°C are shown in Fig. 8. After 96 h, the substrate was completely degraded to irregular particles.

The surface morphologies of coated samples are shown in Fig. 9. The surfaces of both samples were covered by corrosion product layers; however, the corrosion product layer on the ZnN-coated sample was uniform, while on the CaN-coated sample the corrosion products were distributed in clusters (Fig. 9a, 9b).

The chemical composition analysis (EDX) presented in Fig. 10 revealed a significant difference in the chemical composition of the surface corrosion products studied. From the substrate surface (Fig. 10a, 10b), high-intensity peaks of Mg and O were identified. EDX analysis indicated the presence of Na, Cl, Ca and Zn. On the surface of CaN and ZnN samples, high-intensity peaks of O and Mg were identified, and EDX analysis indicated the presence of Cl, Zn and Ca.

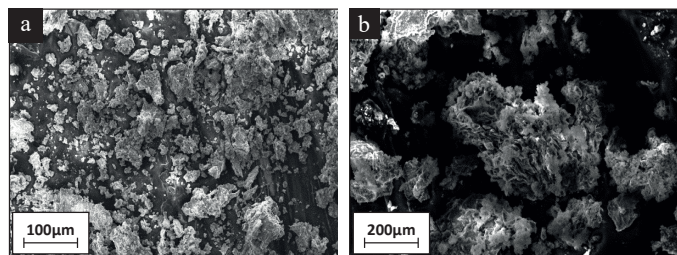


Fig. 8. SEM images of residual Mg49Zn4Ca sample after immersion tests in Ringer's solution at 37°C: a) magnification 90×, b) magnification 500×

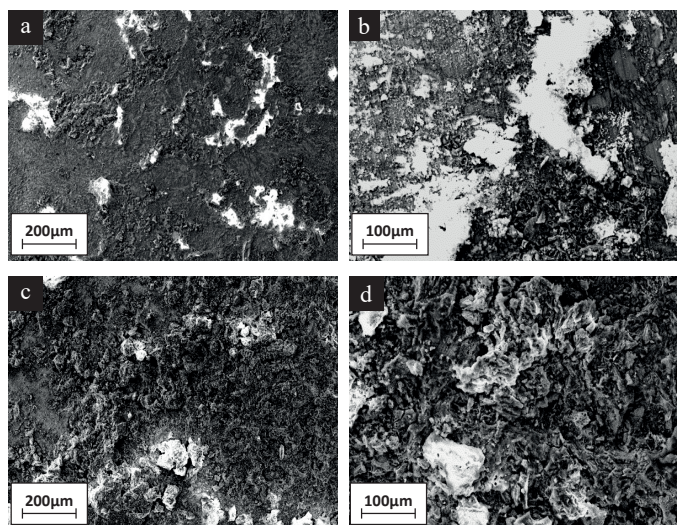


Fig. 9. SEM images of sample surface morphology of (a, b) Mg49Zn4Ca + CaN coating and (c, d) Mg49Zn4Ca + ZnN coating after immersion tests in Ringer's solution at 37°C

a)	Element	Wt%	At%	b)	Element	Wt%	At%
	OK	20.0	31.6		CK	12.4	22.4
	NaK	19.6	21.5		OK	30.0	40.7
	MgK	25.7	26.6		MgK	26.0	23.2
	ClK	19.7	14.0		ClK	1.9	1.1
	CaK	1.5	0.9		CaK	11.7	6.3
	ZnK	13.2	5.1		ZnK	17.8	5.9
	Matrix	Correction	ZAF		Matrix	Correction	ZAF

c)	Element	Wt%	At%
	OK	30.9	46.4
	MgK	44.1	43.5
	ClK	0.8	0.5
	CaK	2.4	1.4
	ZnK	21.6	7.9
	Matrix	Correction	ZAF

Fig. 10. Chemical composition analysis (EDX) of: a) Mg49Zn4Ca, b) Mg49Zn4Ca + CaN coating, and c) Mg49Zn4Ca + ZnN coating after immersion tests in Ringer's solution at 37°C

4. Discussion

Analysis of the microscopic observations of the substrate (Fig. 1, 2) showed that the structure of the MgZn49Ca4 alloy consisted of three phases: Mg, Ca₂Mg₆Zn₃, and Mg₁₂Zn₁₃. This multiphase structure negatively affects the corrosion resistance of magnesium alloys, as confirmed by the results of corrosion resistance tests in this work. The results of immersion and electrochemical tests indicated lower corrosion resistance of the substrate as compared with the coated samples. The hydrogen evolution rate (Fig. 6b) of the substrate increased with immersion time. For coated samples, the hydrogen evolution rates are more stable. The stable hydrogen release rate of samples with CaN and ZnN coatings was associated probably with a homogeneous coating structure. The substrate with a three-phase structure may corrode at different rates in different areas. The penetration of chlorides from Ringer's solution occurred most easily at interphases and at pores in the intrinsically-formed oxide layer. A magnesium oxide layer formed on magnesium alloys, but it was porous because the molar volume of magnesium oxide was smaller than the molar volume of the equivalent amount of magnesium (Pilling-Bedworth coefficient is 0.81), and the oxide film formed was not hermetic [27]. After immersion in an aqueous solution (Ringer's solution) the oxide layer changed from a magnesium hydroxide layer, which is also porous [28].

Therefore, there is a need to create a uniform protective layer on the surface of magnesium alloys. In the case of coated samples, the corrosion rate is similar over the whole surface; therefore, the hydrogen release rate is also similar during the 96 h immersion, except for the first 24 h of immersion, in which the coated samples and the substrate must adapt to new environmental conditions. Hydrogen was released from locations where chlorides damaged the oxide layer (in the case of the substrate) or coating (in the case of the ZnN and CaN-coated samples). The release of hydrogen is a cathodic reaction during the corrosion of magnesium alloys. Qin *et al.* [29] and Srinivasan [30] found that a higher cathodic current density in the polarization curves accelerated the cathodic process of hydrogen release for the magnesium alloys studied. The test results confirmed higher cathodic electrochemical activity of the substrate as compared with coated samples. The cathodic part of the potentiodynamic curve of the Mg49Zn4Ca alloy was located in the high current range, which indicated high cathodic activity (Fig. 7a). The cathodic part of the potentiodynamic curve of the coated samples was located in a lower current range, which indicated lower cathodic activity than the substrate. In addition, changes in the open-circuit potential as a function of time (Fig. 7b) for the substrate were very large. The E_{OCP} potential was unstable, probably due to the high activity of the cathodic (hydrogen release) and anodic (ion release of alloy components) reactions of the substrate. Anodic reactions will likely lead to the release and subsequent growth of a corrosion product layer. These may be associated with the selective release of active metals, which are alloy components (Mg, Ca), and which thus increase the concentration of more electropositive

zinc in the alloy. This, in turn, allows the progression of pitting corrosion on the sample substrate.

The open-circuit potential of ZnN-coated samples showed slight fluctuations, but the E_{OCP} fluctuations were much smaller in both coated samples. For the CaN sample, E_{OCP} was also more stable than that of the substrate, but it shifted to negative values. This indicates a lower corrosion resistance of the CaN sample than of the ZnN sample, implying non-uniform corrosion. Post-immersion SEM images of the substrate and coated samples (Figs. 8, 9) confirmed that pitting corrosion during substrate immersion probably led to complete disintegration of the substrate, and non-uniform corrosion of the coated samples, especially the CaN sample, was caused by unevenly distributed products on the sample surface. The coated samples created more stable layers of corrosion products; therefore, rebuilding of the corrosion product layer was slower than that of the substrate. The denser the layers of corrosion products, the higher the corrosion resistance. The ZnN coating provided better corrosion protection because the corrosion product layer on the ZnN-coated sample was uniform, while the corrosion products on the CaN-coated sample were distributed in clusters (Figs. 9a, b). It should also be mentioned that the better protective properties of the compact ZnN coating, together with corrosion products, were confirmed by the measured Cl concentration on the samples following immersion in Ringer's solution (Fig. 10). The Cl concentration of the substrate was nearly 20 wt% and about 1 wt% for the coated samples. High concentrations of Na and Cl were found in the substrate because it was completely degraded. On the other hand, in the case of coated samples, the concentration of chlorine (about 1 wt%) proves that the coatings, together with the corrosion product layer formed during immersion, created an effective barrier against corrosion.

The EDS results (Figs. 3, 5a, 5b) and the chemical composition of the RCaN coating solution (Table 1) show that the CaN coating consisted mainly of sodium nitrate and/or calcium hydroxide. Sodium nitrate is commonly used to preserve food. In dentistry, calcium hydroxide is used as a base for filling a tooth defect. This information concerns each substance separately. However, it is not certain that they will not become toxic when combined in the human body. For this purpose, cytotoxicity tests need to be performed.

The EDS results (Figs. 3, 5a, 5b) and the chemical composition of the RCaN coating solution (Table 1) show that the CaN coating consisted mainly of sodium nitrate and/or calcium hydroxide. The coating formed on the surface of the MgZn49Ca4 alloy after immersion in the RZnN solution showed more homogeneous morphology than the coating on the CaN sample. The EDS results (Fig. 4, 5c, 5d) and the chemical composition of the RZnN solution (Table 1) show that the ZnN coating consisted mainly of zinc oxide and/or sodium nitrate.

ZnO coatings on magnesium alloys in the literature have been used to increase biological activity (accelerating the formation of apatite on a sample surface) and to give anti-bacterial properties to Mg alloy and ZnO coating systems [31]. Accordingly, magnesium alloys with a ZnO coating may have a ben-

eficial effect on the progress and degradation mechanisms, as shown in this work.

5. Conclusion

Based on the analysis of the research results, the following conclusions were made: ZnN coating provided better corrosion protection because the corrosion product layer on the ZnN-coated sample was uniform, while the sample with a CaN coating showed corrosion products distributed in clusters; the coated samples created more stable corrosion product layers; therefore, the rebuilding of the corrosion product layer was slower than that of the substrate. As more dense corrosion product layers formed, corrosion resistance increased. Pitting corrosion during substrate immersion led to complete disintegration of the substrate, and non-uniform corrosion of the coated samples, especially the CaN sample, was caused by unevenly-distributed products on the sample surface. However, the study analyzes the corrosion mechanisms of the tested materials. On the basis of the tests performed, it was concluded that the coating, especially on the ZnN sample, protects against chloride penetration as long as it is uniform. However, if the thickness of the coating changes with the time of immersion and its continuity is broken by chlorides, there is a chance that a layer of corrosion products will be formed at this point, which will also temporarily protect against further corrosion damage. This is possible due to the large amount of metallic Zn in the alloy, which has very low solubility in aqueous solutions. Due to the immersion time (only 96 hours), there is a possibility that the coating only affects the initial corrosion rate in the first days of immersion, but maybe does not significantly affect the corrosion rate of the implant in the long term. Long-term studies should be performed to confirm the hypothesis.

The ZnN coating probably consisted of zinc oxide and/or sodium nitrate. The ZnN coating on Mg alloys has a beneficial effect on the progress and degradation mechanisms. A literature review shows that zinc compounds, in particular ZnO, can provide antibacterial properties and increase the biological activity of coated magnesium alloys [31, 32]; therefore, further research on ZnN samples will be conducted by the author to assess the bioactivity and antibacterial properties of the produced ZnN layers on magnesium alloys to obtain bioactive and resorbable materials for short-term orthopedic implants.

REFERENCES

- [1] K. Kowalski and M. Jurczyk, "Porous magnesium based bionanocomposites for medical application", *Arch. Metall. Mater.* 60(2), 1433–1435, (2015).
- [2] A. Milenin, M. Gzyl, T. Rec, and B. Plonka, "Computer aided design of wires extrusion from biocompatible mg-ca magnesium alloy", *Arch. Metall. Mater.* 59(2), 551–556 (2014).
- [3] F. Witte, N. Hort, C. Vogt, S. Cohen, K.U. Kainer, R. Willumeit, and F. Feyerabend, "Degradable biomaterials based on magnesium corrosion", *Curr. Opin. Solid. State Mater. Sci.* 12, 63–72 (2008).

- [4] S. Kumar, D. Kumar, and J. Jain, "Surface and interface characteristics of CeO₂ doped Al₂O₃ coating on solution treated and peak aged AZ91 Mg alloy", *Surf. Coat. Tech.* 332, 511–521 (2017).
- [5] Z. Xu, U. Eduok, and J. Szpunar, "Effect of annealing temperature on the corrosion resistance of MgO coatings on Mg alloy", *Surf. Coat. Tech.* 357, 691–697 (2019).
- [6] Y. Gao, L. Zhao, X. Yao, R. Hang, and B. Tang, "Corrosion behavior of porous ZrO₂ ceramic coating on AZ31B magnesium alloy", *Surf. Coat. Tech.* 349, 434–441 (2018).
- [7] R. Ji, M. Ma, Y. He, C. Liu, and J. Wu, "Improved corrosion resistance of Al₂O₃ ceramic coatings on AZ31 magnesium alloy fabricated through cathode plasma electrolytic deposition combined with surface pore-sealing treatment", *Ceram. Int.* 44, 15192–15199 (2018).
- [8] P. Liu, X. Pan, W. Yang, K. Cai, and Y. Chen, "Al₂O₃-ZrO₂ ceramic coatings fabricated on WE43 magnesium alloy by cathodic plasma electrolytic deposition", *Mater. Lett.* 70, 16–18 (2012).
- [9] J. V. Rau, I. Antoniac, M. Filipescu, C. Cotrut, and M. Dinescu, "Hydroxyapatite coatings on Mg-Ca alloy prepared by Pulsed Laser Deposition: Properties and corrosion resistance in Simulated Body Fluid", *Ceram. Int.* 44, 16678–16687 (2018).
- [10] S. Jiang, S. Cai, Y. Lin, X. Bao, and G. Xu, "Effect of alkali/acid pretreatment on the topography and corrosion resistance of as-deposited CaP coating on magnesium alloys", *J. Alloys. Compd.* 793, 202–211 (2019).
- [11] J. G. Acheson, S. McKillop, P. Lemoine, A. R. Boyd, and B. J. Meenan, "Control of magnesium alloy corrosion by bioactive calcium phosphate coating: Implications for resorbable orthopaedic implants", *Materialia* 6, 1–10 (2019).
- [12] P. Shi, B. Niu, E. Shanshan, Y. Chen, and Q. Li, "Preparation and characterization of PLA coating and PLA/MAO composite coatings on AZ31 magnesium alloy for improvement of corrosion resistance", *Surf. Coat. Tech.* 262, 26–32 (2015).
- [13] S. Manna, A. M. Donnell, N. Kaval, and F. Marwan, "Improved design and characterization of PLGA/PLA-coated Chitosan based micro-implants for controlled release of hydrophilic drugs", *Int. J. Pharm.* 547(1–2), 122–132 (2018).
- [14] L. Li, L. Cui, R. Zeng, S. Li, and M. Bobby Kannan, "Advances in functionalized polymer coatings on biodegradable magnesium alloys – A review", *Acta Biomater.* 79, 23–36 (2018).
- [15] Y. Lin, S. Cai, S. Jiang, D. Xie, and G. Xu, "Enhanced corrosion resistance and bonding strength of Mg substituted β -tricalcium phosphate/Mg(OH)₂ composite coating on magnesium alloys via one-step hydrothermal method", *J. Mech. Behav. Biomed.* 90, 547–555 (2019).
- [16] H. R. Bakhsheshi-Rad, E. Hamzah, A. F. Ismail, M. Aziz, and A. Chami, "In vitro degradation behavior, antibacterial activity and cytotoxicity of TiO₂-MAO/ZnHA composite coating on Mg alloy for orthopedic implants", *Surf. Coat. Tech.* 334, 450–460 (2018).
- [17] H. Reza, B. Rad, A. Fauzi Ismail, M. Aziz, Z. Hadisi, and X. Chen, "Antibacterial activity and corrosion resistance of Ta₂O₅ thin film and electrospun PCL/MgO-Ag nanofiber coatings on biodegradable Mg alloy implants", *Ceram. Int.* 45, (9), 11883–11892 (2019).
- [18] E. Yılmaz, B. Çakıroğlu, A. Gökçe, F. Findik, and M. Özacar, "Novel hydroxyapatite/graphene oxide/collagen bioactive composite coating on Ti16Nb alloys by electrodeposition", *Mater. Sci. Eng.: C* 101, 292–305 (2019).
- [19] M. Nowak, B. Płonka, A. Kozik, M. Karaś, M. Mitka, and M. Gawlik, "Conversion coatings produced on az61 magnesium alloy by low-voltage process", *Arch. Metall. Mater.* 61, 419–424 (2016).
- [20] R. Zen, G. Sun, Y. Song, F. Zhang, S. Li, H. Cui, and E. Han, "Influence of solution temperature on corrosion resistance of Zn-Ca phosphate conversion coating on biomedical Mg-Li-Ca alloys", *Trans. Nonferrous. Met. Soc. China* 23(11), 3293–3299 (2013).
- [21] W. Zai, X. Zhang, Y. Zhao, H. C. Man, G. Li, and J. Lian, "Comparison of corrosion resistance and biocompatibility of magnesium phosphate (MgP), zinc phosphate (ZnP) and calcium phosphate (CaP) conversion coatings on Mg alloy", *Surf. Coat. Tech.* 397, 1–17 (2020).
- [22] N. Van Phuong and S. Moon, "Comparative corrosion study of zinc phosphate and magnesium phosphate conversion coatings on AZ31 Mg alloy", *Mater. Lett.* 122, 341–344 (2014).
- [23] Z. Gao, X. Li, and S. Jiang, "Current status, opportunities and challenges in chemical conversion coatings for zinc", *Colloid Surface A* 546, 221–236 (2018).
- [24] J. Hofstetter, M. Becker, E. Martinelli, A. M. Weinberg, B. Mingler, H. Kilian, S. Pogatscher, P. J. Uggowitzer, and J. F. Löffler, High-Strength Low-Alloy (HSLA) Mg–Zn–Ca alloys with Excellent Biodegradation Performance, *JOM* 66(4), 566–572 (2014).
- [25] S. Wasur-Rahman, and M. Medraj, "Critical assessment and thermodynamic modeling of the binary Mg–Zn, Ca–Zn and ternary Mg–Ca–Zn systems", *Intermetallics* 17, 847–864 (2009).
- [26] S. Kim, Y. Kim, Y. K. Lee, and M. Lee, "Determination of ideal Mg–35Zn–xCa alloy depending on Ca concentration for biomaterials", *J. Alloys Compd.* 766, 994–1002 (2018).
- [27] P. Dudek, A. Fajkiel, T. Reguła, and K. Saja, "Selected problems of a technology of the AZ91 magnesium alloy melt treatment", *Prace Instytutu Odlewnictwa, zeszyt 1, Tom XLIX*, 27–42 (2009).
- [28] M. Liu, P. Schmutz, P. J. Uggowitzer, G. Song, and A. Atrens, "The influence of yttrium (Y) on the corrosion of Mg–Y binary alloys", *Corros. Sci.* 52, 3687–3701 (2010).
- [29] F. Qin, G. Xie, Z. Dan, S. Zhu, and I. Seki, "Corrosion behavior and mechanical properties of Mg–Zn–Ca amorphous alloys", *Intermetallics* 42, 9–13 (2013).
- [30] A. Srinivasan, C. Blawert, Y. Huang, C. L. Mendis, K. U. Kainer, and N. Hort, "Corrosion behavior of Mg–Gd–Zn based alloys in aqueous NaCl solution", *J. Magnes. Alloys.* 2, 245–256 (2014).
- [31] J. Sunb, S. Cai, Q. Li, Z. Li, and G. Xu, "UV-irradiation induced biological activity and antibacterial activity of ZnO coated magnesium alloy", *Mater. Sci. Eng.: C* 114, 1–9 (2020).
- [32] H. R. Bakhsheshi-Rad, E. Hamzah, A. F. Ismail, M. Aziz, M. Kasisiri-Asgarani, and H. Ghayour, "In vitro corrosion behavior, bioactivity, and antibacterial performance of the silver-doped zinc oxide coating on magnesium alloy", *Mater. Corros.* 68, 1228–1236 (2017).